PHYSICAL REVIEW B

CONDENSED MATTER

THIRD SERIES, VOLUME 34, NUMBER 10 15 NOVEMBER 1986

Simultaneous epitaxy and substrate out-diffusion at a metal-semiconductor interface: Fe/GaAs(001)-$c(8\times2)$

S. A. Chambers, F. Xu, H. W. Chen, I. M. Vitomirov, S. B. Anderson, and J. H. Weaver

Department of Chemical Engineering and Materials Science, University of Minnesota, Minneapolis, Minnesota 55455

(Received 11 July 1986)

We have combined high-angular-resolution Auger-electron diffraction, kinematical scattering calculations, low-energy-electron diffraction (done in a pulse-counting mode), and high-energy-resolution x-ray photoelectron spectroscopy to examine the formation of the Fe/GaAs(001)-$c(8\times2)$ interface. We find that clusters of bcc Fe at least three atomic layers deep grow in registry with the substrate for coverages up to ~4 monolayer equivalents. These clusters contain Ga and As atoms which have been liberated from the GaAs substrate. Above this coverage, the clusters coalesce into a continuous bcc Fe matrix with a lattice constant equal to half that of GaAs and with principal crystallographic axes parallel to those of the substrate. This epitaxial Fe overlayer contains Ga and As in solution in the bcc lattice with the impurity atoms occupying interstitial face-center sites. The concentration of Ga and As decreases with distance from the GaAs substrate. At the same time, we find clear evidence for surface segregation of As and enrichment of the near-surface region.

The possibility of growing thin, epitaxial single crystals with unique magnetic properties has attracted considerable scientific and technological interest.[1–18] Of particular interest is the role the substrate plays in determining the structural, electronic, and magnetic properties of the supported film. For example, it has recently been suggested, on the basis of total electronic energy calculations, that ultrathin films of Cr, V, and Fe grown on nonmagnetic substrates might exhibit enhanced magnetism.[6,7] These calculations indicate significantly different magnetic coupling in interfacial thin films relative to the bulk. At the same time, the structural details of strained overlayers resulting from overlayer-substrate lattice misfit is virtually unexplored,[19] and its role in perturbing magnetic coupling is not known.

Recent investigations of Fe and Co overlayers on GaAs(110) have revealed that epitaxial growth occurs and that body-centered-cubic (bcc) films of both metals can be grown.[1–5] The α phase of Fe, which exists at room temperature, has a bcc structure with a lattice constant of 2.86 Å. GaAs possesses a zinc-blende structure with a lattice constant of 5.65 Å. Thus, it is possible to mesh these two structures together with a lattice misfit of 1.24% by doubling the number of Fe atoms per unit area at the interface relative to the number of substrate atoms in the surface layer. That Co grows epitaxially on GaAs(110) to form a bcc phase is highly unusual and very intriguing because Co normally assumes a hexagonal-close-packed structure (hcp) at room temperature. However, as Prinz has shown, it is possible to predict on the basis of the lattice parameter versus composition curve for the Co-Fe system that if a metastable bcc phase of Co could be synthesized, it would probably have a lattice constant of ~2.82 Å. A bcc film with this lattice constant would grow epitaxially on GaAs with a misfit of only 0.2%, and such growth appears to be the case for the (110) orientation of GaAs.[5] Furthermore, recent high-resolution synchrotron radiation photoemission results indicate that Fe promotes Ga and As out-diffusion when deposited onto cleaved GaAs(110) surfaces.[20]

The simultaneous occurrence of both epitaxy and surface disruption leading to out-diffusion makes these systems highly unusual and very interesting. Indeed, it appears that they are ideal testing grounds for our understanding of the parameters which control epitaxy, disruption, and intermixing. In order to investigate these issues, we have used high-energy Auger-electron diffraction, low-energy-electron diffraction (LEED), and high-resolution x-ray photoelectron spectroscopy (XPS) to probe the structure and composition of the interface formed by depositing Fe overlayers on reconstructed GaAs(001)-$c(8\times2)$. Combined with kinematical scattering calculations, these experimental probes provide us with detailed information about the nature of the Fe overlayer as it develops from ultralow coverages to higher coverages.

Angle-resolved Auger and low-energy-electron diffraction measurements were performed in a spectrometer op-

timized for interface studies, as described elsewhere.[21] 5-kV electrons were used to excite the $L_3M_{4,5}M_{4,5}$ Auger transitions of Fe, Ga, and As at 700, 1066, and 1222 eV, respectively. LEED spectra were obtained by simultaneously ramping the primary electron beam voltage and cylindrical mirror analyzer (CMA) mirror voltage so as to always analyze the elastic peak and by applying a 1.5-V peak-to-peak modulation to the analyzer mirror voltage to avoid drifting off the elastic peak maximum as the beam energy is swept. Complementary measurements were conducted in a second chamber equipped with conventional Auger and LEED optics.

XPS measurements were performed with a Surface Science Laboratories SSX-100-03 x-ray photoelectron spectrometer employing monochromatized Al k_α x radiation (1486.6 eV). The emphasis of the present photoemission studies was on the Fe $3p$, the Ga $3d$, and the As $3d$ core electrons. All core level spectra were obtained with a pass energy of 50 eV and an x-ray beam diameter of 300 μm. Spectra were also taken as a function of collection angle which was measured relative to the surface plane. The half-angle of acceptance of the analyzer was 15°, resulting in a cone of acceptance of 30°.

Si-doped GaAs(001) wafers oriented to within 0.5° of (001) were etched in a mixture of H_2O_2, H_2SO_4, and H_2O (5:5:1) prior to insertion into any of the spectrometers. Once under UHV conditions (4×10^{-11} Torr), the wafers were cleaned with the following procedure: Ar-ion sputtering at 500 eV ion energy and 8 μA ion beam current until the residual carbon was removed (≤ 10 min of sputter time); simultaneous sputtering (125 eV and 3 μA) and annealing at 390 °C for 90 min; and final annealing at 500 °C for 30 min. Repetitive cycles produced a well-ordered GaAs(001)-$c(8\times2)$ reconstruction with little or no residual carbon.

Fe evaporations were done by resistively heating a W boat containing pieces of electron-beam-purified Glidden Fe. The Fe sources were extensively outgassed prior to the measurements, and deposition of Fe could be done with the system pressures below 2×10^{-10} Torr. The metal flux was monitored by means of a quartz crystal oscillator, the typical source to sample distance was 30 cm, and the deposition rate was typically 1 Å per minute. Coverages are reported in monolayers (ML) of Fe on an unreconstructed, Ga-terminated GaAs(001) surface (6.27×10^{14} atoms/cm^2), hereafter referred to as monolayer equivalents.

Cluster scattering calculations were performed within the kinematical or single-scattering approximation[22] on a Cray Research, Inc. Cray II supercomputer made available through the University of Minnesota Supercomputer Institute. We used free-atom scattering factors and phase shifts[23,24] and empirical reductions of scattering factors and inelastic mean free paths by 50%, as discussed elsewhere.[25–27] Different crystal structures were assumed for the Fe overlayer. Each structure was modeled as a cluster of 100 Fe atoms per layer for comparison with experimental data. These 100 atom layers were found to yield fully convergent results.

In Fig. 1 we show the reciprocal and possible real space geometries for the GaAs(001)-$c(8\times2)$ and bcc Fe(001)

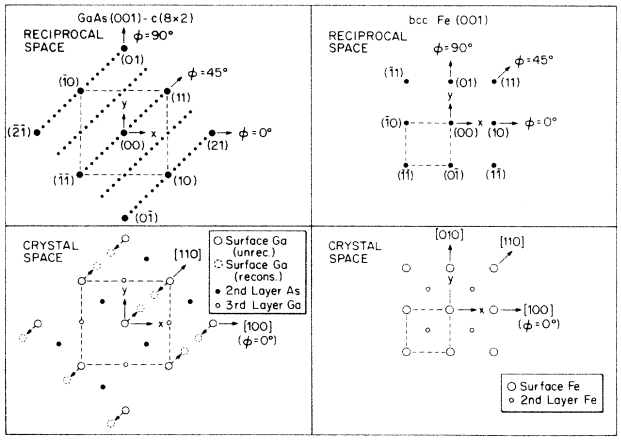

FIG. 1. Reciprocal and crystal space diagrams for the surfaces of GaAs(001)-$c(8\times2)$ and α-phase bcc Fe(001) extracted from LEED patterns for GaAs(001)-$c(8\times2)$ with and without Fe overlayers. The [001] directions of substrate and overlayer were found to be parallel, indicating that Fe growth occurs in the orientation which maximizes the lattice match.

surfaces, along with our choice of coordinate system for the problem. In each case, the reciprocal space geometry shown at the top of the figure was observed in the LEED patterns for the clean substrate and for Fe overlayers with coverages in excess of ~5 ML. The real space geometry of Ga-terminated GaAs(001)-$c(8\times2)$ is not yet known, but it seems plausible that the reconstruction is driven by the tendency of two dangling bonds per surface Ga atom to form bridge bonds with neighboring Ga atoms. The projections of these sp^3 hybrid bonds into the plane of the surface make an angle of 45° with respect to the principal crystallographic axes of the surface fcc unit cell. The direction of doubled periodicity in reciprocal space is also at 45° with respect to fcc mesh, suggesting a surface structure which contains rows of bridge bonds as shown in the lower left-hand panel of Fig. 1.

It is important to note that the [100] direction of the Fe overlayer was found to be parallel to that of the substrate, showing that the bcc Fe surface mesh and the fcc GaAs mesh have parallel sides. This orientation can be accommodated with a lattice match of 98.75% by doubling the number of Fe atoms per unit area relative to that for the surface layer of Ga.

In order to probe the details of the overlayer geometry, we present in Fig. 2 polar-angle intensity distributions of Fe $L_3M_{4,5}M_{4,5}$ Auger emission in the (010) azimuthal plane ($\phi=0°$) as a function of coverage in monolayer equivalents on GaAs(001). The (010) azimuthal plane was located experimentally by collecting LEED I-V spectra as a function of azimuthal angle and locating the (21) beam from the substrate (Fig. 1). At 1 and 2 ML equivalents, a diffraction-induced feature appears at a polar angle (θ) of ~40°. By 3 ML equivalents a second feature appears at $\theta=90°$ (normal emission). These two features grow in intensity and become narrower with coverage. Also, the feature at ~40° shifts to higher polar angle and reaches a constant value of 45° by a coverage of 7 ML equivalents.

Additional structure grows in at $\theta=20°$ and $\theta=60°-70°$ as the overlayer develops. However, there are no substantial changes from 8 ML equivalents to 68 ML equivalents (not shown). The significance of the diffraction-induced maxima along [101] and [001] is that they can be associated directly with the presence of chains of atoms along those vectors. Atoms closer to the surface act as forward scatters of Auger electrons emitted from atoms in lower layers. Therefore, we conclude that the Fe overlayer has grown by 3 ML equivalents in such a way that cubic arrays of atoms exist and at least two layers of atoms are aligned to allow forward scattering along [001]. We will discuss the peak near [101] later.

In Fig. 3 we show LEED I-V spectra as a function of coverage for diffracted beams in the (010) and ($\bar{1}$10) azimuthal planes. Also shown at the top of the figure is the experimental geometry used to obtain the spectra. The sample was set for normal incidence for the electron beam generated by the coaxial gun in the energy analyzer, and elastic peak intensities were collected as a function of primary energy in the two azimuthal planes. The features at 43 eV (left panel top curve) and 23 eV (right panel top curve) in (001) and ($\bar{1}$10) are assigned to the (21) and (11) beams from the substrate, respectively. These assignments are made by using the Bragg law expressed for incident beam scattering at our scattering angle of 138° ($\pi-42°$). The resulting expression, which relates the kinetic energy of the (hk) LEED beam in eV [$K(h,k)$] to the associated surface reciprocal lattice vector $\mathbf{G}(h,k)$ in Å^{-1} is given by

$$K(h,k)=8.52n^2\,|\,\mathbf{G}(h,k)\,|^2\,, \tag{1}$$

where n is the order of the beam. Using Eq. (1), the first-order (21) and (11) beams for GaAs(001) are predicted to occur at 42 and 21 eV, respectively, in very good agreement with the observed values of 42 and 23 eV. The additional features seen for the clean surface in the ($\bar{1}$10) plane are due to the $c(8\times2)$ reconstruction.

As Fe is deposited, the diffracted beams associated with the substrate surface layer weaken, the background increases, and three additional beams abruptly appear at 3 ML equivalents at 48 and 190 eV in (010) and at 91 eV in ($\bar{1}$10). These features are assigned to diffracted beams associated with strained α-phase bcc Fe whose lattice constant is expected to be 2.82 Å on a GaAs substrate. Using

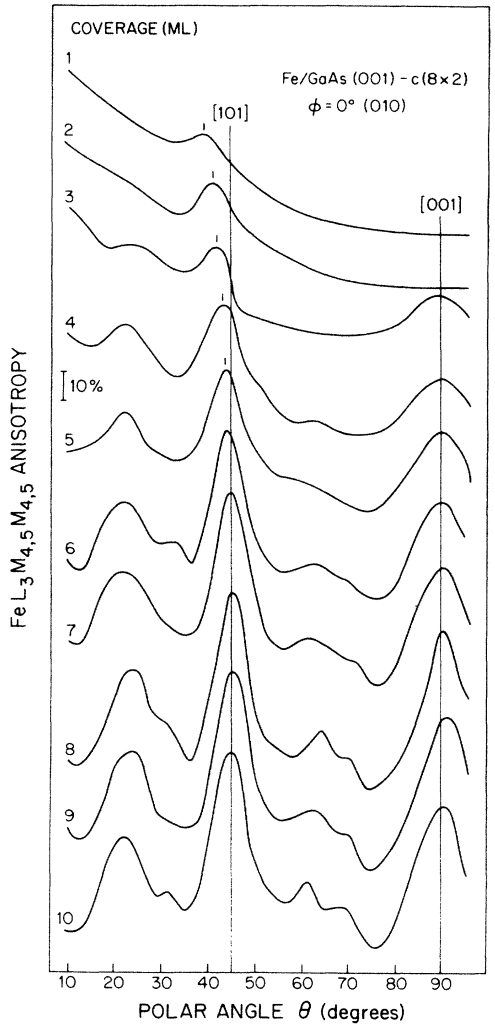

FIG. 2. Fe $L_3M_{4,5}M_{4,5}$ Auger polar-angle intensity distributions in the (010) azimuthal plane of the GaAs substrate as a function of Fe coverage. The appearance of diffraction-induced maxima at $\theta=40°-45°$ and $\theta=90°$ indicates the presence of scattering centers along these directions relative to Fe atoms in the interfacial layer.

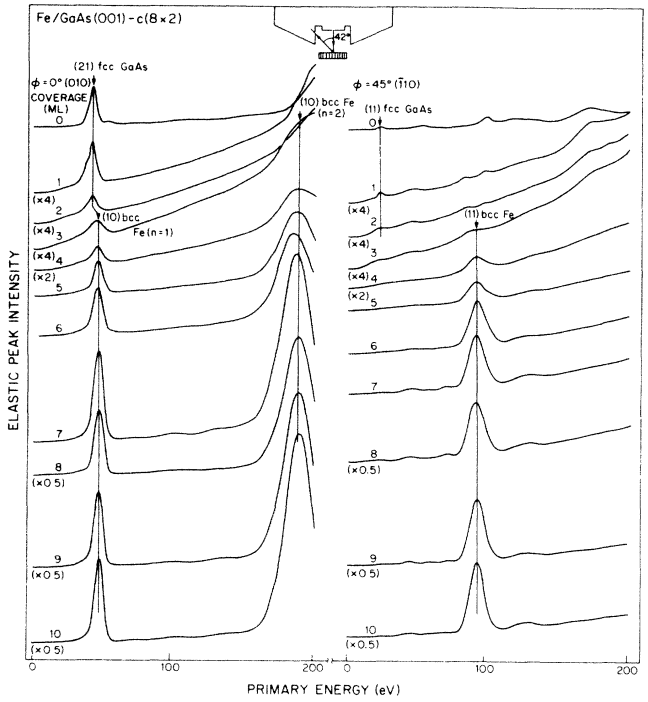

FIG. 3. LEED I-V spectra obtained for a fixed scattering angle of 138° in the (010) and ($\bar{1}$10) azimuthal planes. Peak assignments were made on the basis of Eq. (1), which relates LEED beam kinetic energy to the associated reciprocal lattice vector (see text).

Eq. (1) we predict that if this phase grows epitaxially on GaAs(001), it will generate LEED beams at 42 and 168 eV associated with first- and second-order diffraction of the (10) beam in (010), respectively, and at 84 eV for first-order diffraction of the (11) beam in ($\bar{1}$10). Moreover, epitaxy requires that the (10) beams occur in the (010) azimuthal plane of the substrate while the (11) beam should occur in ($\bar{1}$10), as is observed. These diffracted beams grow in intensity and sharpen as coverage proceeds. Therefore, we conclude that despite the $c(8\times2)$ reconstruction, Fe is able to grow epitaxially on GaAs(001) as a bcc film and that the principal crystallographic axes of the overlayer are parallel to those of the substrate.

This structure assignment has important implications for the coverage calibration and, therefore, conclusions drawn about the mode of growth at low coverages. The α phase of Fe has a lattice constant which is approximately half that of GaAs. Therefore, a coverage of 1 ML equivalent of Fe on GaAs(001) represents enough atoms of only *one half* of the surface to be covered with a layer of bcc Fe. Therefore, the coverages used in Figs. 1 and 2 should be divided by two to obtain the actual coverage expressed in terms of monolayers of Fe in the bcc phase. Returning to Fig. 2 we see that a diffraction feature occurs at $\theta=90°$ (normal emission) for a coverage of 3 ML equivalents (1.5 ML of bcc Fe). Due to the forward-focusing nature of electron-atom scattering at the kinetic energy of Fe $L_3M_{4,5}M_{4,5}$ Auger emission (700 eV), this feature can only occur if a *third* layer of Fe atoms is present. These atoms would then act as forward scatterers for the first-layer Fe atoms. In order for a third layer to develop when only enough atoms for 1.5 ML of bcc have been deposited, cluster formation must be occurring. This conclusion is further supported by LEED spectra at low coverage, particularly those in ($\bar{1}$10) which betray the $c(8\times2)$ reconstruction. In Fig. 4 we show detailed LEED spectra in the ($\bar{1}$10) azimuthal for very low Fe coverages. We now express the coverage in terms of layers of Fe present in the bcc form. As seen in Fig. 4, the (11) LEED beam associated with GaAs(001)-$c(8\times2)$ is clearly present up to 2 ML [4 ML equivalents on GaAs(001)], which exceeds the coverage by which a three-layer-deep bcc Fe phase has formed according to Auger diffraction results. Taken together, these results demonstrate that

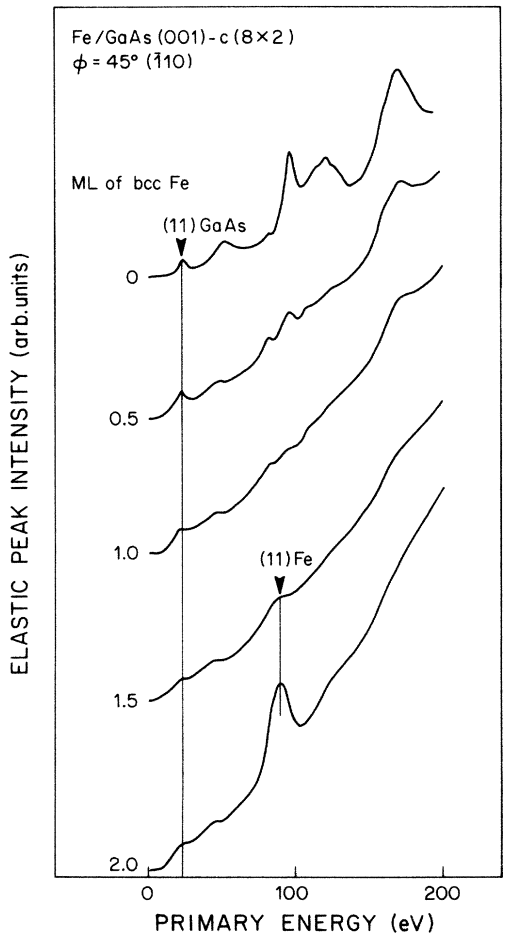

FIG. 4. Vertically expanded LEED *I-V* spectra in the ($\bar{1}$10) azimuthal plane showing the simultaneous existence of clusters of bcc Fe and patches of unperturbed substrate.

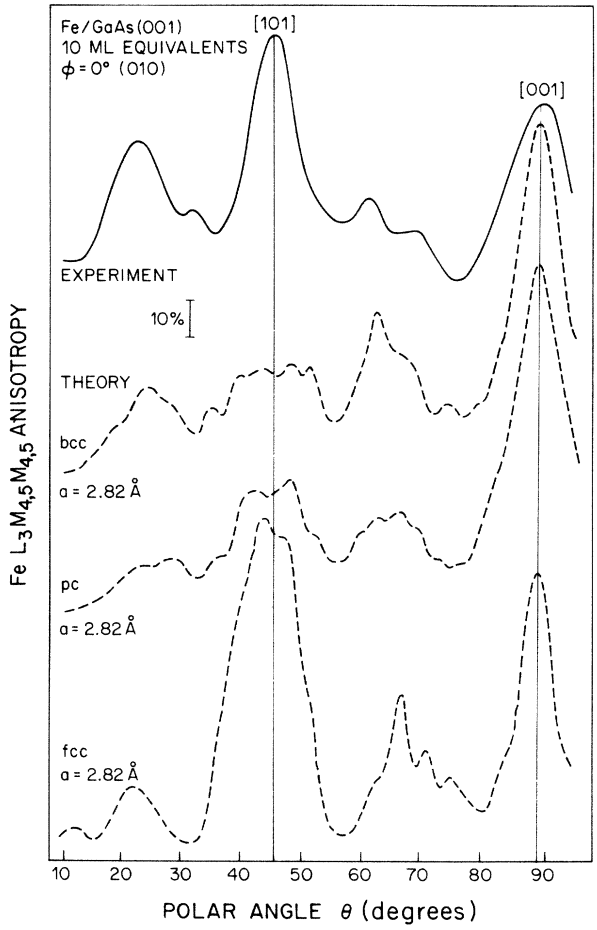

FIG. 5. Measured and calculated Fe $L_3M_{4,5}M_{4,5}$ polar-angle intensity distributions for various model structures of 10 ML equivalents of Fe on GaAs(001)-$c(8\times2)$.

clusters of bcc Fe whose lateral dimensions are sufficiently large to coherently diffract the incident LEED beam are present together with patches of uncovered substrate.

In order to further examine the structural nature of the Fe overlayer, we show in Fig. 5 a comparison of experimental Fe $L_3M_{4,5}M_{4,5}$ Auger polar-angular distributions for 10 ML equivalents of Fe on GaAs(001)-$c(8\times2)$ with calculations in which different crystal structures were assumed. The Fe phase diagram shows that the bcc α phase of Fe is stable for temperatures below 1160 K and low pressure. However, for pressures in excess of 100 kbar and temperatures below 940 K, and hcp ϵ phase forms, and an fcc γ phase forms for high temperature and high pressure. A triple point for these three phases is observed at 770 K and 110 kbar.[28] It is conceivable that the 1.24% lattice compression of Fe needed for epitaxial growth on GaAs(001) could force the overlayer into a metastable hcp phase. However, we have no evidence whatsoever that this occurs. The γ phase is not likely to form at room temperature, and a primitive cubic structure does not occur naturally for Fe. Nevertheless, we have performed calculations for an fcc Fe structure forced into registry with the substrate, primitive cubic (pc) Fe, and the more likely bcc Fe for comparison with experiment.

The results shown in Fig. 5 reveal excellent agreement between theory and experiment for the forced fcc structure and marginal agreement for the pc and bcc structures. The forced fcc structure successfully predicts major intensity maxima along [101] and [001] whereas the pc and bcc models underestimate the intensity of the peak along [101], due to the absence of scatterers at the face-centered sites. The structure at $\theta=60°-70°$ is better accounted for in the bcc calculation than in the others. While the agreement between theory and experiment is superior for the simple forced fcc Fe structure, there are two reasons to question its legitimacy. First, the measured LEED spectra are incompatible with an fcc surface periodicity. Equation (1) predicts the presence of (21) and (11) beams at 165 and 82 eV, respectively, if a forced Fe fcc structure exists. As in the case of substrate scattering, the (21) and (11) beams should fall in the (010) and ($\bar{1}$10) azimuthal planes, respectively. Although a beam is observed at 91 eV in ($\bar{1}$10) which may be the (11) beam of the fcc structure, there is no peak at 165 eV in (010). However, the appearance of a beam at 48 eV in (010) is expected if the surface unit cell is the (001) face of an Fe bcc structure. Therefore, the LEED spectra are consistent with a bcc surface mesh, but not with a fcc surface structure. A second reason to question the simple forced fcc Fe structure is that the density would be twice that of the α phase which ordinarily forms at room temperature. Therefore, Fe is not expected to assume this structure. We are therefore led to postulate the possibility of foreign atoms occupying interstitial sites of face-centered character in a bcc Fe lattice. Such a structure would account for the LEED and Auger diffraction data discussed so far by leaving the primitive bcc surface mesh intact and positioning atoms in face-centered sites within the Fe matrix. These atoms would give rise to an Auger diffraction peak along [101]. In order to cause minimal strain on the Fe lattice, these foreign atoms must have a smaller atomic radius than Fe and be able to easily fit into these interstitial sites. Moreover, the foreign atoms should have scattering strengths comparable to those of Fe, in order to produce an Auger angular distribution similar to what is expected from the hypothetical forced fcc Fe structure (shown in Fig. 5). The obvious source of such atoms is the substrate. Therefore, we turn to high-resolution XPS results to see if, in fact, Ga and As atoms have diffused into the Fe overlayer.

In Fig. 6, we show normalized Ga and As $3d$ core level emission spectra as a function of Fe coverage expressed in ML of bcc Fe. These spectra were collected at 15° grazing emission in order to enhance the sensitivity of XPS to the near-surface region. (The maximum probing depth is estimated to be $\sim$30 Å at this emission angle.) By a coverage of 0.34 ML, both the Ga and As core lines show a broadening to lower binding energy due to reaction with the Fe adatoms. This broadening becomes more pronounced with coverage. For Ga, we can see a well-defined second peak. Line-shape decomposition into two Gaussians shows that this new feature moves in energy away from the substrate position (estimated position 0.8 eV at 0.34 ML and 1.1 eV at 20 ML). Analogous line-shape decomposition for the As $3d$ emission was not successful with the relatively poor resolution of the present studies. In contrast, Ruckman *et al.* decomposed higher-resolution synchrotron-radiation photoemission data for the Fe/GaAs(110) system into three As $3d$ components.[20]

In Fig. 7 we plot the total reduced Ga and As $3d$ emission intensities (defined as $\ln[I(d)/I(0)]$, where d is the overlayer thickness) as a function of coverage. At low

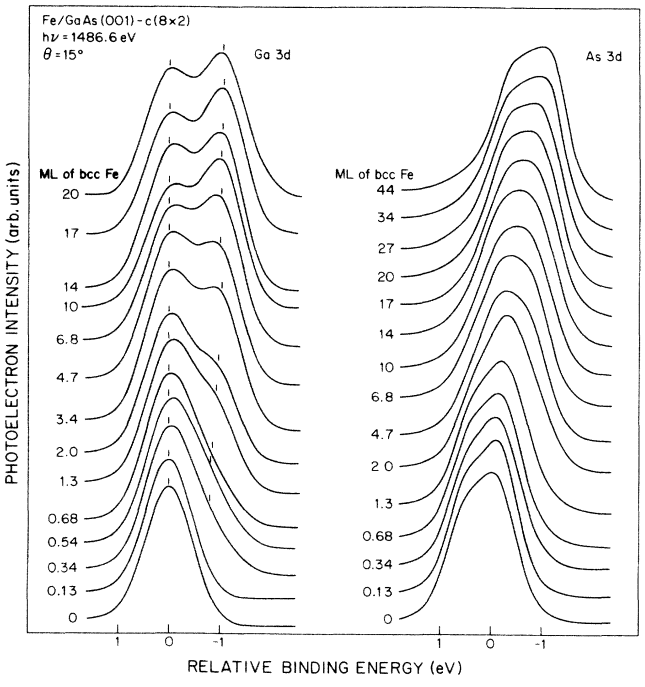

FIG. 6. High-resolution Ga and As $3d$ photoelectron spectra excited by monochromatized Al k_α radiation (1486.6 eV) as a function of Fe coverage. The collection angle was 15° with respect to the surface plane.

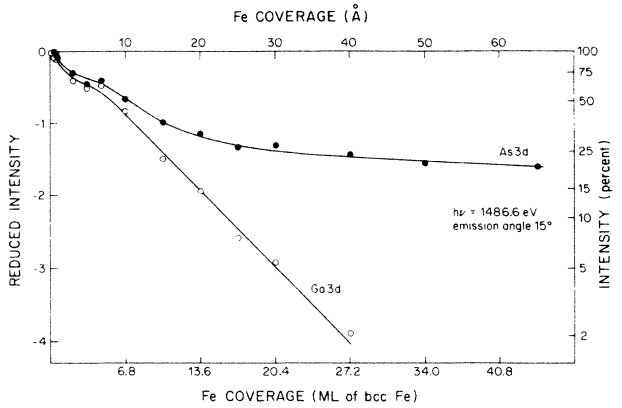

FIG. 7. Ga and As $3d$ reduced intensity (defined as $\ln[I(d)/I(0)]$, where d is the overlayer thickness) vs Fe coverage expressed in both ML of bcc Fe and angstroms.

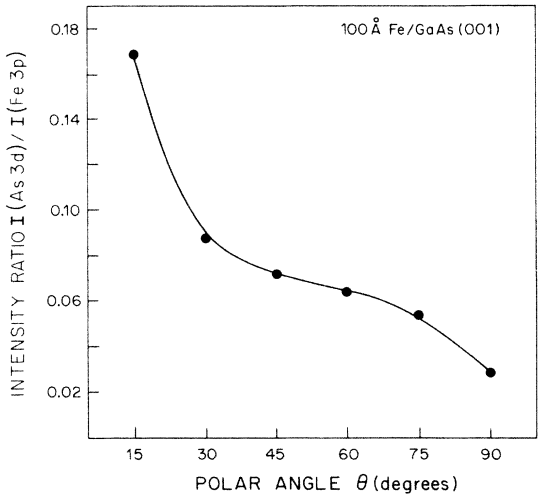

FIG. 8. As $3d$ to Fe $3p$ photoelectron intensity ratio vs collection angle for a coverage of 100 Å. The rise with decreasing angle indicates the presence of surface-segregated As.

coverage, the Ga and As emission diminishes rather sharply. The attenuation curves exhibit inflection near 3—4 ML coverage, and emission from both Ga and As then decreases with increasing coverage, with the rate of Ga attenuation being much greater than that of As above about 12 ML. The results of Figs. 6 and 7 clearly establish the out-diffusion of both Ga and As with the extent of As out-diffusion being greater, in agreement with results for the Fe/GaAs(110).[20] The Auger-electron diffraction data of Figs. 2 and 5 indicate that these out-diffused substrate atoms are present in the face-center intersitital sites of the Fe bcc lattice.

Our XPS results and those of Ruckman *et al.* show that As is present in the probed region long after the Ga content is negligible. Since the disruption of the substrate liberates Ga and As in approximately equal amounts (baring an exchange reaction), one must ask about the spatial distribution of the As in the interfacial region. In order to determine whether the As content of the probed region is homogeneous or whether there is surface segregation, we have performed polar-angle-resolved XPS measurements of the As $3d$ and Fe $3p$ intensities after 100 Å of Fe had been deposited onto GaAs(001). At this coverage, there is no residual contribution from the substrate, even in normal emission, as evidenced by the absence of any Ga $3d$ emission. In Fig. 8 we plot the ratio of the As $3d$ to the Fe $3p$ emission as a function of polar angle. This intensity ratio increases as the emission angle decreases and the measurements emphasize the surface region. Therefore, we conclude that some fraction of the As visible at high coverages is indeed surface-segregated As. Recalling that the LEED spectra indicated that the surface mesh is the (001) face of a bcc structure with a lattice constant of ~ 2.8 Å, we suggest that the surface-segregated As atoms are in registry with the Fe overlayer.

The picture which emerges from these results is that the Fe/GaAs interface forms a well-ordered Fe bcc phase with out-diffused As and Ga atoms in interstitial sites and an enrichment of As in the surface region. The overlayer is then an Fe crystal with a solid solution of semiconductor atoms dissolved in the metal matrix. As a check of this model, we investigated the Fe $3p$ spectra as a function of coverage collected at $\theta = 15°$ to enhance emission from the top 30 Å of the overlayer. These results (not shown) indicate that the Fe $3p$ core level steadily shifts to lower binding energy with increasing coverage. The total shift is ~ 0.5 eV between submonolayer and 20 ML coverage. These results are consistent with the behavior of the Ga binding energy, which also showed a steady shift with increasing coverage corresponding to increasing dilution. Simple initial-state charge transfer arguments suggest that a high Ga and/or As concentration in a Fe matrix would increase the Fe $3p$ binding energy relative to bulk Fe, and that the Fe $3p$ binding energy would decrease as the semiconductor atom concentration decreases.

The electronic structure and the magnetic properties of this Fe-based overlayer should be quite different from those of bulk Fe. Indeed, Prinz *et al.* have performed magnetic measurements for Fe/GaAs(001) and have observed marked magnetic anisotropies for Fe coverages up to 700 Å.[29] These anisotropies may be due to either lattice strain or semiconductor impurity atoms. Since both phenomena occur due to pseudomorphic growth on GaAs with Ga and As diffusion into the Fe matrix, it is quite likely that both phenomena influence the magnetic coupling in the overlayer.

The conclusions drawn here about the composition of the overlayer differ somewhat from those by Ruckman *et al.*[20] for the Fe/GaAs(110) interface. With the superior resolution afforded by synchrotron radiation, they fitted the As $3d$ core levels with three distinct doublets corresponding to the substrate, an As-Fe compound, and the solid solution, finding that the spatial extent of the compound was only a few angstroms and its chemical shift relative to the substrate was 0.4 eV. Given the present structural information for the interface at low Fe coverages, it is possible that this Fe-As compound should be thought of instead as a slightly different chemical environment for As in the ultrathin transition region from

substrate to Fe overlayer. The final environment is ultimately the solution phase of As in bcc Fe, as discussed by Ruckman *et al.*, and the broad As $3d$ emission represents the superposition of a number of chemically inequivalent sites. In essence, an epitaxial solid solution model would then be supported by the photoemission data at both levels of resolution (XPS and synchrotron radiation). In any event, it is clear that Fe adatoms have a minimally disruptive effect on the GaAs surface. Bonds are indeed broken, allowing substrate atoms to diffuse into the overlayer. However, this process does not occur sufficiently to destroy the template necessary for epitaxy.

In summary, we have shown that Fe overlayers on GaAs(001)-$c(8\times2)$ nucleate as α-phase bcc Fe in registry with the substrate at low coverage and that these clusters coalesce into a continuous film at higher coverages. The Fe film contains out-diffused Ga and As atoms in the face-centered interstitial sites of the bcc lattice, and As segregates to the surface region producing an interface with heterogeneous As content. The $c(8\times2)$ reconstruction, whose structure is not yet known, does not prevent the growth of bcc Fe.

This work was supported by the National Science Foundation under Grants Nos. DMR-82-16489 and DMR-86-10837. The calculations were done on the Cray II supercomputer at the University of Minnesota Supercomputer Institute. The authors are pleased to acknowledge helpful conversations with G. A. Prinz, J. J. Joyce, and M. W. Ruckman.

[1]G. A. Prinz and J. J. Krebs, Appl. Phys. Lett. **39**, 397 (1981).
[2]G. A. Prinz, G. T. Rado, and J. J. Krebs, J. Appl. Phys. **53**, 2087 (1982).
[3]C. Vittoria, F. J. Rachford, J. J. Krebs, and G. A. Prinz, Phys. Rev. B **30**, 3903 (1984).
[4]K. Schröder, G. A. Prinz, K.-H. Walker, and E. Kisker, J. Appl. Phys. **57**, 3669 (1985).
[5]G. A. Prinz, Phys. Rev. Lett. **54**, 1051 (1985).
[6]C. L. Fu, A. J. Freeman, and T. Oguchi, Phys. Rev. Lett. **54**, 2700 (1985).
[7]C. L. Fu and A. J. Freeman, Phys. Rev. B **33**, 1611 (1986).
[8]C. L. Chien, S. H. Liou, D. Kofalt, W. Tu, T. Egami, and T. R. McGuire, Phys. Rev. B **33**, 3247 (1986).
[9]B. J. Thaler, J. B. Ketterson, and J. E. Hilliard, Phys. Rev. Lett. **41**, 336 (1978).
[10]T. Jarlborg and A. J. Freeman, Phys. Rev. Lett. **45**, 653 (1980).
[11]R. Miranda, F. Yuduráin, D. Chandesris, and J. Lecante, Surf. Sci. **117**, 319 (1982).
[12]L. E. Klebanoff, S. W. Robey, G. Liu, and D. A. Shirley, Phys. Rev. B **30**, 1048 (1984).
[13]R. Miranda, F. Yuduráin, D. Chandesris, J. Lecante, and Y. Petroff, Phys. Rev. B **25**, 527 (1982).
[14]S. Ohniski, M. Weinert, and A. J. Freeman, Phys. Rev. B **30**, 36 (1984).
[15]J. Tersoff and L. M. Falicov, Phys. Rev. B **26**, 6186 (1982).
[16]E. Wimmer, A. J. Freeman, and H. Krakauer, Phys. Rev. B **30**, 3113 (1984).
[17]D.-S. Wang, A. J. Freeman, and H. Krakauer, Phys. Rev. B **24**, 1126 (1981).
[18]J. Tersoff and L. M. Falicov, Phys. Rev. B **25**, 2959 (1982).
[19]S. A. Chambers, H. W. Chen, I. M. Vitomirov, S. B. Anderson, and J. H. Weaver, Phys. Rev. B **33**, 8810 (1986).
[20]M. W. Ruckman, J. J. Joyce, and J. H. Weaver, Phys. Rev. B **33**, 7029 (1986).
[21]S. A. Chambers and L. W. Swanson, Surf. Sci. **131**, 385 (1983).
[22]See C. S. Fadley, in *Progress in Surface Science*, edited by S. G. Davision (Pergamon, New York, 1984), Vol. 16, pp. 327–340 for an excellent discussion of the model employed here.
[23]D. Gregory and M. Fink, At. Data Nucl. Data Tables **14**, 39 (1974).
[24]M. Fink and J. Ingram, At. Data **4**, 129 (1972).
[25]M. Saguraton, E. L. Bullock, R. Saiki, A. Kaduwela, C. R. Brundle, C. S. Fadley, and J. J. Rehr, Phys. Rev. B **33**, 2207 (1986).
[26]R. Trehan and C. S. Fadley, J. Electron Spectrosc. Relat. Phenom. (to be published).
[27]S. Y. Tong, H. C. Poon, and D. R. Snider, Phys. Rev. B **32**, 2096 (1985).
[28]F. P. Bundy, J. Appl. Phys. **36**, 616 (1965).
[29]G. A. Prinz (private communication).